symmetry

MDPI

Article

Orientation Dependence of High-Order Harmonic Generation from HeH^{2+} in a Corotating Two-Color Circularly Polarized Laser Field

Na Gao [1,2], Yue Qiao [1,2], Yuan Wang [1,2], Jun Wang [1,2,*], Fuming Guo [1,2,*] and Yujun Yang [1,2,*]

[1] Institute of Atomic and Molecular Physics, Jilin University, Changchun 130012, China
[2] Jilin Provincial Key Laboratory of Applied Atomic and Molecular Spectroscopy, Jilin University , Changchun 130012, China
* Correspondence: wangjun86@jlu.edu.cn (J.W.); guofm@jlu.edu.cn (F.G.); yangyj@jlu.edu.cn (Y.Y.)

Abstract: By numerically solving the time-dependent Schrödinger equation, we study high-order harmonic generation from the asymmetric diatomic molecule HeH^{2+} in a corotating two-color circularly polarized laser field. Our results reveal a strong correlation between the molecule orientation and the harmonic yield. The harmonics in the plateau region can achieve an intensity modulation of one to two orders of magnitude with the change in the orientation angle. Through the time-dependent evolution of ionized electron wave packets combined with the analysis of the transition dipole moment between the continuum and bound states, the modulation of the harmonic strength may be attributed to the difference in the recollision angle of ionized electron wave packets relative to the molecules. In addition, the harmonic ellipticity is also affected by the molecular orientation. Notably, we found that the harmonic with greater ellipticity and higher intensity can be obtained with an orientation angle of 147°. These findings open up new avenues for achieving enhanced efficiency, the near-circular polarization of harmonics, and precise control over harmonic polarization states.

Keywords: orientation dependence; high-order harmonic; ellipticity; transition dipole

Citation: Gao, N.; Qiao, Y.; Wang, Y.; Wang, J.; Guo, F.; Yang, Y. Orientation Dependence of High-Order Harmonic Generation from HeH^{2+} in a Corotating Two-Color Circularly Polarized Laser Field. *Symmetry* **2024**, *16*, 185. https://doi.org/10.3390/sym16020185

Academic Editor: Wiesław Leonski

Received: 2 January 2024
Revised: 24 January 2024
Accepted: 1 February 2024
Published: 4 February 2024

1. Introduction

High-order harmonic generation (HHG) is an interesting nonlinear phenomenon observed in the interaction of intense laser pulses with atoms, molecules, and solids [1–7]. The semiclassical three-step model can well describe the mechanism of HHG [8]. The first step is that the bound electrons have a certain probability of ionization from the ground state under the influence of the laser field. In the second step, the liberated electrons undergo oscillatory motion in the laser field. Finally, when the laser field is reversed, part of the electron wave packets has the opportunity to return to the nuclear region to recombine with the parent ion and emit high-energy photons [9,10]. Owing to the spectral coverage ranging from ultraviolet to soft X-ray, HHG is an efficient means of obtaining attosecond pulses, which can detect and track the ultrafast dynamics of intramolecular electrons. Therefore, it has gradually been attracting more attention [11–16].

Compared with atoms, molecules with more complex structures will produce richer physical phenomena in the HHG process, such as orientation effects [17,18], two-center interference effects [19,20], multiorbital effects [21,22], and so on. For asymmetric molecules with permanent dipole moments, such as CO [23], HeH^{2+} [24], and LiH^{3+} [25], the charges are mainly located on the heavier nuclei, which is different from symmetric molecules. The laws and mechanisms of HHG are more complex, so the study of asymmetric molecules is also of great significance. Asymmetric molecules have been studied in depth, and it has been found that molecular orientation has a great impact on HHG [26–28]. In 2011, Bian and Bandrauk studied the interaction of monochromatic linearly polarized laser pulses with HeH^{2+}. Their results show that when the molecular axis is along the laser polarization

direction, the obtained harmonic intensity is the largest, surpassing the harmonic intensity obtained when the molecular axis is perpendicular to the laser polarization direction by more than two orders of magnitude. This phenomenon is attributed to the role of the molecular structure and excited states [29]. In 2017, based on time-dependent density functional theory, Hu et al. reported the HHG of CO molecules in a linearly polarized laser field and confirmed that even pure harmonics were generated when the molecular axis was perpendicular to the laser polarization direction [30].

It is well known that the generation efficiency of HHG is very sensitive to the dependence of the ellipticity of the driving laser [31–34]. The current research mainly uses a linearly polarized driving field. Under this driving laser, the intensity of HHG is the highest. Owing to the wide application of circularly polarized HHG in magnetic materials, chiral materials [35–37], and so on, the obtaining of circularly polarized harmonics with high efficiency is the focus of current research. Therefore, the regulation of HHG polarization characteristics with two-color circular polarization has attracted more and more attention. In the past few years, it has been observed experimentally that when the counter-rotating two-color circularly polarized laser pulses interact with atoms and molecules, a strong circularly polarized harmonic radiation can be generated, because the ionized electrons driven by this pulse can return to the parent ion at different angles [38]. Theoretically, Qiao et al. observed a certain intensity of harmonic radiation by using the interaction between the corotating two-color circular polarization (CRTCCP) laser field and the H_2^+ molecule and found that the ellipticity of the specific harmonic order changes with the molecule orientation angle [39]. In order to further explore the complex dynamics of asymmetric molecules in strong laser fields, whether the harmonics generated by the CRTCCP laser pulse will depend on the molecular orientation and the influence of molecular orientation on harmonic efficiency and ellipticity is the focus of this work.

In this paper, we investigate the orientation dependence of HHG from HeH^{2+} irradiated by the CRTCCP laser pulse through numerical simulations based on the time-dependent Schrödinger equation (TDSE). In the second part of this paper, the theoretical method for calculating the harmonic spectrum is introduced, and the third part shows the results and related discussion and analysis. We summarize our research work in the last part, and atomic units are used throughout this article unless specified otherwise.

2. Model and Methods

Under electric dipole approximation and length gauge, we numerically calculate a two-dimensional TDSE of the HeH^{2+} driven by a CRTCCP laser field:

$$i\frac{\partial}{\partial t}\psi(\vec{r},t) = [-\frac{1}{2}\nabla^2 + V(\vec{r}) + \vec{E}(t)\cdot\vec{r}]\psi(\vec{r},t). \quad (1)$$

The soft-core Coulomb potential of the nucleus perceived by the electron is

$$V(\vec{r}) = -\frac{Q_1}{\sqrt{r_1+A}} - \frac{Q_2}{\sqrt{r_2+A}}, \quad (2)$$

here, $r_1 = (x - R_1\cos\theta)^2 + (y - R_1\sin\theta)^2$, $r_2 = (x + R_2\cos\theta)^2 + (y + R_2\sin\theta)^2$, $R_1 = Q_2R/(Q_1+Q_2)$, and $R_2 = Q_1R/(Q_1+Q_2)$ represent the position of the He and the H nuclei and Q_1 = 2 and Q_2 = 1 are the charges for the He and H nuclei. R = 4 a.u. is the nuclear distance. θ is the angle between the molecular axis and x axis. A = 0.65 is the soft-core parameter. The I_p =1.03 a.u. is for $2p\sigma$ orbitals in HeH^{2+} [40,41]. The electric field vector of the CRTCCP pulse $\vec{E}(t) = \vec{E}_1(t) + \vec{E}_2(t)$ is the superposition of two circularly polarized laser beams, which can be expressed as

$$\vec{E}_1 = E_0 f(t)\left[\cos(\omega_0 t)\hat{e}_x + \sin(\omega_0 t)\hat{e}_y\right],$$

$$\vec{E}_2 = E_0 f(t)\left[\cos(2\omega_0 t)\hat{e}_x + \sin(2\omega_0 t)\hat{e}_y\right], \quad (3)$$

$\hat{e}_x$ ($\hat{e}_y$) is the unit vector along the x (y) axis, the $f(t)$ is a trapezoidal envelope function with the total duration of eight optical cycles (o.c.), the time scales of the rising and falling edges are each one cycle of the fundamental frequency, ω_0 is the angular frequency of the fundamental laser pulse, and E_0 is the amplitude of the laser field.

The time-dependent wave function $\psi(\vec{r},t)$ at any instant is obtained by solving Equation (1) with the splitting operator method [42]. In order to prevent unphysical reflection from the wave packet boundary, the wave function is multiplied by the mask function $\cos^{1/8}$ at each time grid point [43]. By using the time-dependent wave function, the dipole accelerations are written as

$$\begin{aligned}\vec{a}(t) &= \langle\psi(\vec{r},t)|-\vec{\nabla}V(\vec{r})-\vec{E}(t)|\psi(\vec{r},t)\rangle \\ &= a_x(t)\hat{e}_x + a_y(t)\hat{e}_y. \end{aligned} \tag{4}$$

Through the Fourier transform, the harmonic spectral components corresponding to the polarization in the x and y directions can be obtained:

$$\begin{aligned} P_x(\omega) &= \left|\frac{1}{\omega^2(t_n-t_0)}\int_{t_0}^{t_n} a_x(t)e^{-i\omega t}dt\right|^2, \\ P_y(\omega) &= \left|\frac{1}{\omega^2(t_n-t_0)}\int_{t_0}^{t_n} a_y(t)e^{-i\omega t}dt\right|^2. \end{aligned} \tag{5}$$

The ellipticity of the HHG is expressed as

$$\varepsilon = (|a_+| - |a_-|)/(|a_+| + |a_-|), \tag{6}$$

where $a_\pm = \frac{1}{\sqrt{2}}(\tilde{a}_x \pm i\tilde{a}_y)$; $\tilde{a}_{x,y} = \int_{-\infty}^{\infty} a_{x,y}(t)e^{-i\omega t}dt$; and $\tilde{a}_x$ and $\tilde{a}_y$ are the components of the dipole acceleration x and y in the frequency domain, respectively [44].

The time-frequency distributions of HHG can be obtained by using the wavelet transformation:

$$A_\omega(t_0,\omega) = \int_{t_{t_s}}^{t_f} a(t)w_{t_0,\omega}(t)dt, \tag{7}$$

$w_{t_0,\omega}(t) = \sqrt{\omega}W[\omega(t-t_0)]$ represents the kernel of the wavelet transform, where $W(x) = (1/\sqrt{\tau})e^{ix}e^{-x^2/2\tau^2}$ is the Morlet's wavelet [45].

3. Results and Discussion

Figure 1 presents the HHG of the HeH^{2+} molecular irradiated by the CRTCCP laser field. The fundamental frequency of the laser pulse is ω_0 = 0.043 a.u., corresponding to a laser wavelength of 1064 nm, and the laser field peak amplitude E_0 is 0.03 a.u. (corresponding to the intensity of 3.16×10^{13} W/cm^2). The HeH^{2+} molecular is in the x-y plane, and the angle (orientation angle) between the molecular axis and the x axis is θ. The angular relationship between the HeH^{2+} molecule and the driving field is shown in Figure 1a. When the orientation angle range varies from 0° to 180°, the variation in the harmonic intensity with the orientation angle is illustrated in Figure 1b. It can be observed that there is a noticeable modulation in the harmonic intensity in the high−energy region as the orientation angle varies. Specifically, within the range of 25th to 35th harmonics, the harmonic intensity at orientation angles between 90° and 120° is significantly stronger than that of other orientation angles. In order to obtain a clearer rule of change, Figure 1c shows the change in single-order harmonics in the plateau with the orientation angle. Both odd and even harmonics appear in the harmonic spectrum, and it can be seen from the figure that the harmonic intensity gradually increases when the orientation angle changes from 0° to 105°, and it does not show a regular trend after θ = 105°. Overall, the harmonic intensity is strongest near θ = 105°, which is about two orders of magnitude higher than the harmonic

intensity at $\theta = 0°$. The previous results demonstrated that the HHG yield of the CRTCCP field is significantly lower than that of the counter−rotating field [46]. Figure 1d shows the harmonic spectra of the counter−rotating (solid black line) and corotating (dash−dotted red line) two-color circularly polarized laser pulses with the same laser parameters and $\theta = 105°$. It can be observed that the harmonic yield is comparable up to the 32nd order.

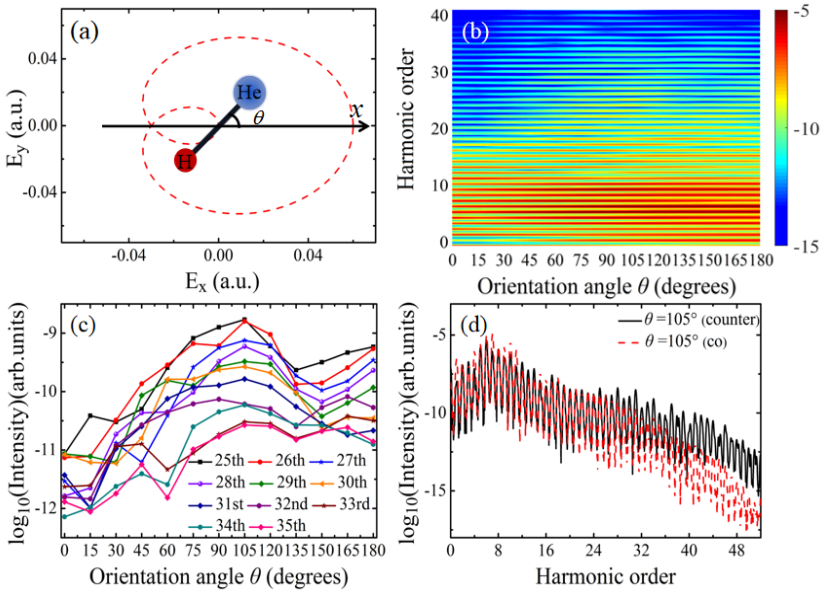

Figure 1. The harmonic spectra of HeH^{2+} in a CRTCCP laser field. (**a**) Schematic diagram of the laser in relation to the angle of the molecule. (**b**) The harmonic intensity changes in HeH^{2+} with different orientation angles. (**c**) Variation in single−order harmonics at different orientation angles of HeH^{2+}. (**d**) $\theta = 105°$, harmonic spectra of HeH^{2+} by the counter−rotating (solid black line) and corotating (dash−dotted red line) two-color circularly polarized laser pulses.

In order to understand the reason for the variation in the harmonic intensity with the molecular orientation angle, we provide the time−frequency analysis of the harmonic emission at two orientation angles of 60° and 105°, as shown in Figure 2a and Figure 2b, respectively. It can be seen that there is a main harmonic emission trajectory in each fundamental frequency optical cycle when the harmonic order is higher than 25th. This phenomenon is different from the electron trajectory of harmonic emission in HeH^{2+} under the case of a linearly polarized field [24]. With a linear polarization pulse, there is a major harmonic emission trajectory every 0.5 optical cycles. In contrast, the harmonic emission with time peaks around $t = (n + 0.7)$ o.c. (n = 1, 2, 3, 4, 5, and 6) by a CRTCCP, and there is a significant difference in the time−frequency characteristics at different orientation angles. A gradual enhancement of the harmonic emission intensity per optical cycle can be observed in Figure 2a. Figure 2b shows that the emission trajectories near $t = (n + 0.7)$ o.c. (n = 2, 3, and 4) are stronger than those in other optical cycles. Furthermore, the harmonic emission in the high−energy region is more intensive at the orientation angle of 105° than at the orientation angle of 60°.

In order to further investigate the harmonic emission behavior and understand the reason for the higher harmonic efficiency of HeH^{2+} at the orientation angle of 105° in a CRTCCP laser pulse, we present the time evolution of electron wave packets at orientation angles of 60° and 105° in Figure 3a and Figure 3b, respectively. To facilitate the analysis of the motion behavior of the wave packet and to better track the phenomenon of electrons returning to the nuclear region, we select a small ionization moment in the case of two orientation angles when each of them can return to the nuclear region and have the highest returning probability. When $\theta = 60°$, we select a small cluster of wave packets that ionized within the time interval from t = 1.04 o.c. to t = 1.10 o.c. for the evolution, and when $\theta = 105°$,

we chose to evolve the ionized wave packets at t = 0.98 o.c. to t = 1.04 o.c. The time interval of ionization under the two orientation angles is the same, both of which are 0.06 o.c. In Figure 3a,b, we give the evolution time period of 1.06 o.c. to 1.69 o.c with an interval of 0.09 o.c. and electric fields at eight corresponding instants $t_1 - t_8$, which are depicted in Figure 3(a1). In addition to the wave packets evolution, in order to follow the motion behavior of the ionized electrons more clearly, the spatial distribution of the electron probability flow velocity was calculated as $\vec{j} = -\frac{i}{2}\left[\psi^*\vec{\nabla}\psi - \psi\vec{\nabla}\psi^*\right]$, where $\vec{\nabla} = \frac{\partial}{\partial x}\vec{i} + \frac{\partial}{\partial y}\vec{j}$, indicated by the arrows in Figure 3. The length of the arrows represents the magnitude of the electron wave packet flow rate, and the direction represents the motion direction of the ionized electron wave packet. Considering that there will be charge migration processes around the nuclear region (shown by the gray circle is the He nuclei, and the red circle is the H nuclei) affecting the observation of the ionized electron wave packet, we removed the electron probability stream in the nuclear region. It can be seen in Figure 3a,b, driven by the CRTCCP laser pulse, that the ionized electron wave packets under the two orientation angles gradually leave the nuclear region and diffuse over time and then follow a counterclockwise direction of motion. Eventually, a portion of the wave packet at θ = 60° returns to the nuclear region at t = 1.69 o.c. And when θ = 105°, some of the wave packets have a tendency to return to the nuclear region at t = 1.60 o.c., and most of the wave packets return to the nuclear region at t = 1.69 o.c. By comparing the ionized electron wave packet evolution at these two orientation angles, we can see that their electron wave packet returns to the nuclear region at significantly different times. In the case of θ = 105°, the ionized electron wave packet returns to the nuclear region with a longer duration. However, when t = 1.69 o.c., the electron wave packet at both orientation angles returns to the nuclear region at the upper left. The recollision direction of the electron wave packet closest to the nuclear region is at an angle of $-75°$ to the x axis. As depicted in Figure 3(b8), the electron wave packet returning to the nuclear region is close to parallel to the molecular axis. Therefore, we conclude that it may be more favorable for the ionized electron wave packet to complex with the bound state when the recollision direction of the electron wave packet is parallel to the oriented molecule, which results in a higher harmonic efficiency at θ = 105°.

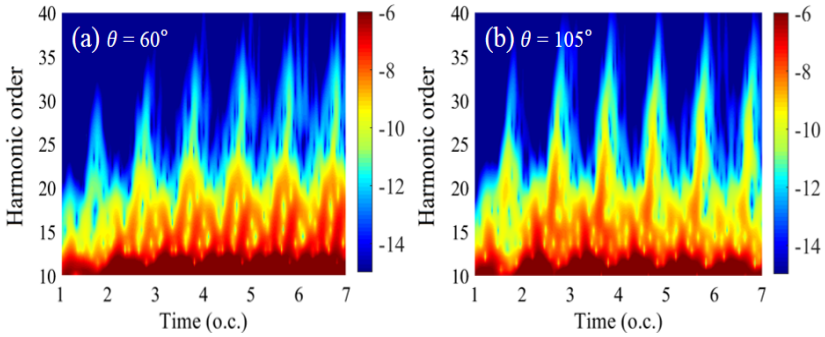

Figure 2. Time−frequency analysis of the harmonic emission when (**a**) θ = 60° and (**b**) θ = 105°.

Based on the above conclusion, the angular relationship between the direction of the electron wave packet back to the nuclear region and the molecular axis is shown in Figure 4a. Here, $\vec{e}$ is the recollision direction of the electron wave packet , and α is the recollision angle. When θ = 0°, α = 105°, and as the orientation angle changes, α changes accordingly. We calculated the transition dipole moment with respect to the direction of electron recombination, which can be expressed as $\vec{d}(p,\alpha) = \vec{d}(p, 105° - \theta) = \langle\psi(\vec{r},\theta)|\vec{e}\cdot\vec{r}|\exp(i\vec{p}\cdot\vec{r})\rangle$ [44], where $\psi(\vec{r},\theta)$ is the time-dependent wave function and $\exp(i\vec{p}\cdot\vec{r})$ is the continuum state. $\vec{p} = \sqrt{2(\omega - I_P)}$ is the momentum of the electron in the recollision direction. Here, I_p is the ionization potential of the system. Figure 4b,c give the variation in the relative dipole strength and harmonic intensity at different orientation angles, respectively. The comparison reveals that the variation in the harmonic yield and the corresponding dipole

intensity are basically the same. The harmonic intensity is stronger when $\theta = 105°$ and the corresponding dipole intensity is also strongest. In Figure 4d,e, the harmonic intensity and corresponding dipole of the 31st and 34th harmonics at different orientation angles are further compared, and it can be seen that the trends of the harmonic intensity and the relative dipole are in good agreement. In summary, the harmonic intensity shows a strong intensity modulation with the molecular orientation angle under the effect of the CRTCCP used in this paper. This is due to the different recollision angles of the molecule. The transition dipole between the continuum state and the bound state is different at different recollision angles. The transition probability is greatest near $\alpha = 0°$ and smallest near $\alpha = 90°$.

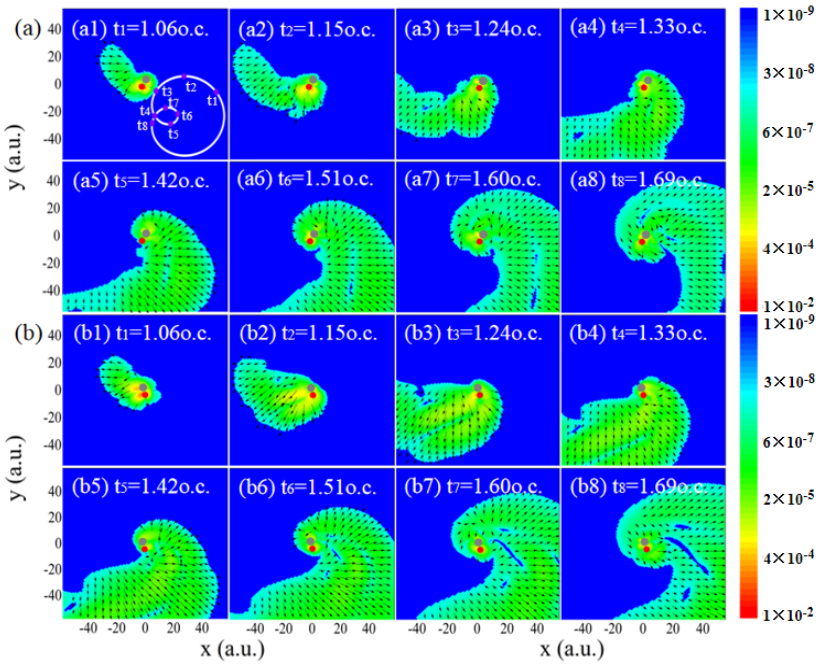

Figure 3. Evolution of the electronic wave packet of HeH^{2+} in a CRTCCP laser pulse for (**a**) $\theta = 60°$ and (**b**) $\theta = 105°$. The corresponding momentary electric field is given in the inset of Figure (**a1**).

After understanding the reason for the stronger harmonic generated at an orientation angle of 105°, we analyze the variation in the harmonic ellipticity with the orientation angle in the plateau region, as shown in Figure 5a, where the color indicates the ellipticity. A 0 indicates linear polarization. The right circular polarization is $+1$, and the left circular polarization is -1. In Figure 5a, it can be seen that the harmonic ellipticity obviously has a large difference at different orientation angles, and the generated harmonics can be converted between different rotations and ellipticities. For the left CRTCCP pulse, it is possible for the direction of the electron to change as the recollision electron is subjected to the force of one of the nuclei, leading to the generation of right circular polarized harmonics. The variation in ellipticity with an orientation angle for the 29th harmonic (blue circular curve) is given in Figure 5b. When the orientation angle is 60°, the ellipticity is -0.71. The ellipticity goes up to 0.92 when the orientation angle is 147°. This means that by changing the orientation angle, we may obtain near−circularly polarized high−order harmonics with higher efficiency. To be able to see more intuitively the polarization properties and rotation of the harmonics at these two orientation angles, we further give the evolution of the harmonic electric field of the 29th harmonic from the HeH^{2+} molecule under a CRTCCP laser field, as shown in Figure 5c,d, where different colors indicate different moments, and we select a small period of optical cycles. The black arrow in the figure points to the rotation direction of the harmonic electric field. We can observe that at $\theta = 60°$, the harmonic electric field is left elliptical polarization. When $\theta = 147°$, the harmonic electric field is right near−circular polarization.

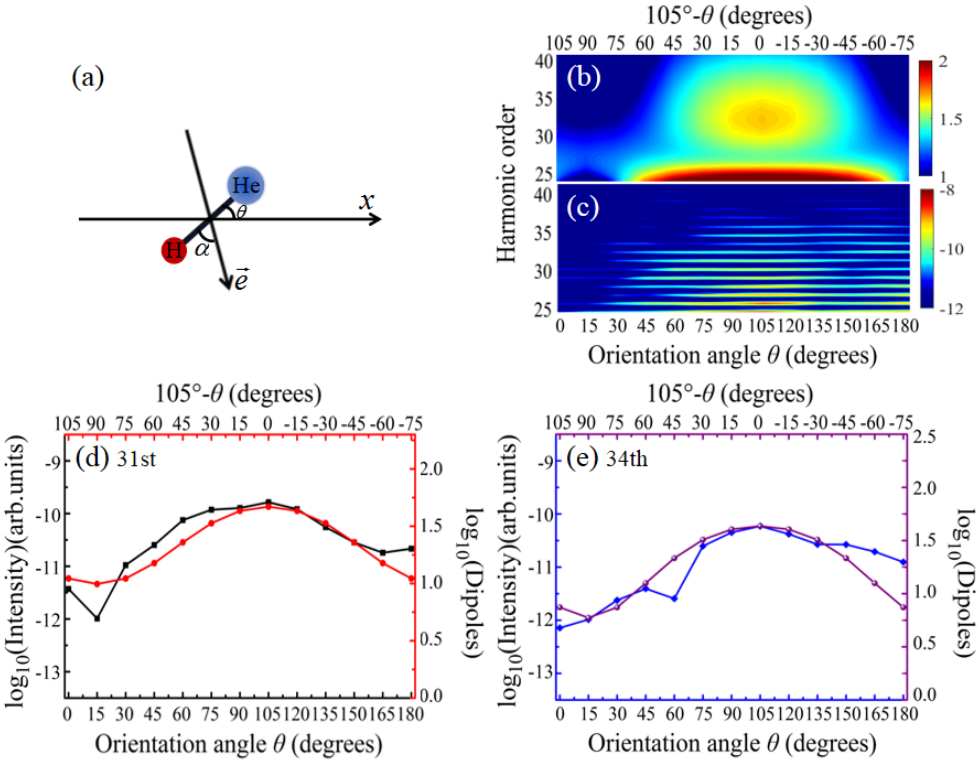

Figure 4. (**a**) Schematic diagram of the electron recombination direction in relation to the molecular orientation angle. (**b**) Relative transition dipole intensity and (**c**) harmonic intensity in the high−energy region change with the orientation angle. (**d**) Variation in harmonic yield (black squares) and corresponding transition dipole (red circles) for 31st harmonic at different orientation angles. (**e**) Variation in the harmonic yield (blue diamond) and the corresponding transition dipole (purple circle) for the 34th harmonic at different orientation angles.

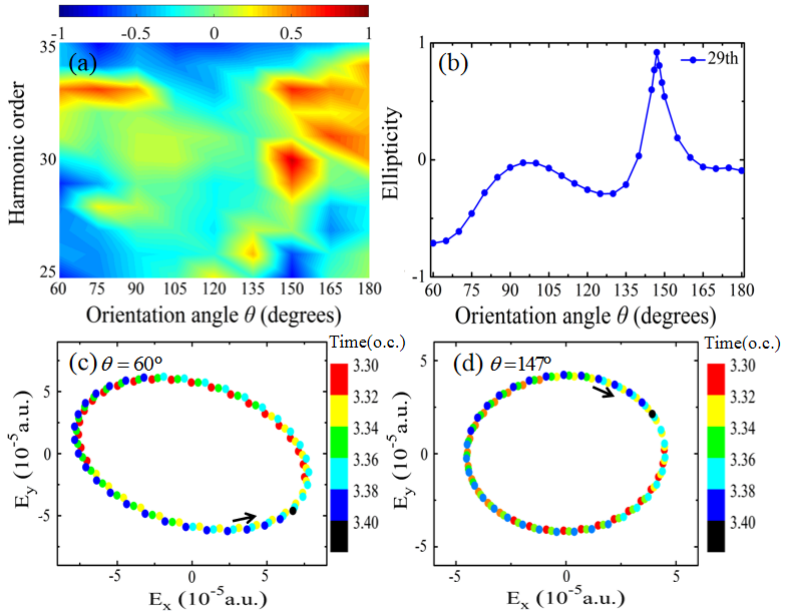

Figure 5. (**a**) Harmonic ellipticity modulation in the plateau region at different orientation angles. (**b**) Harmonic ellipticity variations in 25th (purple circular curve) at different orientation angles. (**c**) θ = 60° and (**d**) θ = 147°, the harmonic electric field of 29th harmonic generated by HeH^{2+} molecules irradiated by CRTCCP fields.

4. Conclusions

In summary, we investigated the harmonic generated by the interaction of a CRTCCP laser pulse with HeH^{2+} molecules. It is observed that the harmonic intensity is very sensitive to the angle between the incident light field and the molecular axis, which is similar to our previous findings for symmetric molecular H_2^+ [39]. However, HHG of the asymmetric molecule HeH^{2+} showed an obvious orientation dependence. The harmonic intensity of $\theta = 105°$ is about two orders of magnitude higher than that of $\theta = 0°$. Through the analysis of time-dependent wave packets, the enhancement is due to the molecular axis at $\theta = 105°$, which is close to parallel to the recollision direction of the ionized electrons, which is more favorable for the electrons to return to the nuclear region. This conclusion has important implications for exploring the structure and dynamics of asymmetric molecules. More importantly, the harmonic polarization state varies with the molecular orientation angle. It is found that harmonic polarization with high ellipticity can be generated at specific orders with orientation angles of 60° and 147°, which could potentially be utilized to generate harmonics with controllable polarization.

Author Contributions: N.G.: data curation, writing original draft, editing, and software. Y.Q.: supervision. Y.W.: supervision. J.W.: supervision. F.G.: conceptualization and supervision. Y.Y.: supervision. All authors have read and agreed to the published version of the manuscript.

Funding: This project was supported by the National Key Research and Development Program of China (grant no. 2019YFA0307700 and no. 2022YFE0134200), the National Natural Science Foundation of China (NSFC; grant no. 12074145, no. 11975012, and no. 12374029), and the Jilin Provincial Research Foundation for Basic Research, China (grant no. 20220101003JC).

Institutional Review Board Statement: Not applicable.

Informed Consent Statement: Not applicable.

Data Availability Statement: The data presented in this study are available upon request from the corresponding author.

Acknowledgments: We acknowledge the High-Performance Computing Center of Jilin University for the supercomputer time and the high-performance computing cluster Tiger@ IAMP.

Conflicts of Interest: The authors declare no conflicts of interest.

References

1. Krausz, F.; Ivanov, M. Attosecond physics. *Rev. Mod. Phys.* **2009**, *81*, 163. [CrossRef]
2. Qiao, Y.; Chen, J.Q.; Huo, Y.Q.; Liang, H.Q.; Yu, R.X.; Chen, J.G.; Liu, W.J.; Jiang, S.C.; Yang, Y.J. Effect of the interference between interband currents on the crystal harmonic spectra. *Phys. Rev. A* **2023**, *107*, 023523. [CrossRef]
3. Lein, M.; Hay, N.; Velotta, R.; Marangos, J.P.; Knight, P. Role of the intramolecular phase in high-harmonic generation. *Phys. Rev. Lett.* **2002**, *88*, 183903. [CrossRef] [PubMed]
4. Telnov, D.A.; Heslar, J.; Chu, S.I. Effect of nuclear vibration on high-order-harmonic generation of aligned H_2^+ molecules. *Phys. Rev. A* **2014**, *90*, 063412. [CrossRef]
5. Yuan, G.; Lu, R.; Jiang, S.; Dorfman, K. Conical Intersection versus Avoided Crossing: Geometric Phase Effect in Molecular High-Order Harmonics. *Ultrafast Sci.* **2023**, *3*, 0040. [CrossRef]
6. Ovchinnikov, A.V.; Chefonov, O.V.; Agranat, M.B. Generation of the Second Optical Harmonic in Silicon under the Action of Terahertz Pulse with High Electric Field Strength. *High Temp.* **2022**, *60*, 607–611. [CrossRef]
7. Khairulin, I.; Antonov, V.; Emelin, M.Y.; Popova, M.; Gryzlova, E.; Ryabikin, M.Y. Multilevel model of multiphoton processes in a helium atom in a strong laser field: Ionization description. *Opt. Spectrosc.* **2023**, *131*, 128–132.
8. Corkum, P.B. Plasma perspective on strong field multiphoton ionization. *Phys. Rev. Lett.* **1993**, *71*, 1994. [CrossRef] [PubMed]
9. Zhang, B.; Lein, M. High-order harmonic generation from diatomic molecules in an orthogonally polarized two-color laser field. *Phys. Rev. A* **2019**, *100*, 043401. [CrossRef]
10. Walker, B.; Sheehy, B.; DiMauro, L.F.; Agostini, P.; Schafer, K.J.; Kulander, K.C. Precision measurement of strong field double ionization of helium. *Phys. Rev. Lett.* **1994**, *73*, 1227. [CrossRef]
11. Bertrand, J.B.; Wörner, H.J.; Hockett, P.; Villeneuve, D.M.; Corkum, P.B. Revealing the Cooper minimum of N_2 by molecular frame high-harmonic spectroscopy. *Phys. Rev. Lett.* **2012**, *109*, 143001. [CrossRef]
12. Ryabikin, M.Y.; Emelin, M.Y.; Strelkov, V.V. Attosecond electromagnetic pulses: generation, measurement, and application. Attosecond metrology and spectroscopy. *Phys. Usp.* **2023**, *66*, 360–380. [CrossRef]

13. Li, X.F.; Qiao, Y.; Wu, D.; Yu, R.X.; Chen, J.G.; Wang, J.; Guo, F.M.; Yang, Y.J. Internal collision double ionization of molecules driven by co-rotating two-color circularly polarized laser pulses. *Chin. Phys. B* **2024**, *33*, 013302. [CrossRef]
14. Sekikawa, T.; Kosuge, A.; Kanai, T.; Watanabe, S. Nonlinear optics in the extreme ultraviolet. *Nature* **2004**, *432*, 605–608. [CrossRef] [PubMed]
15. Yuan, H.Y.; Yang, Y.J.; Guo, F.M.; Wang, J.; Chen, J.G.; Feng, W.; Cui, Z.W. Effect of pulse duration on the above-threshold ionization of a hydrogen atom irradiated by a 400 nm intense laser. *Opt. Exp.* **2023**, *31*, 24213–24229. [CrossRef]
16. Qiao, Y.; Chen, J.; Zhou, S.; Chen, J.; Jiang, S.; Yang, Y. Modulation of high-order harmonic generation from a monolayer ZnO by co-rotating two-color circularly polarized laser fields. *Chin. Phys. Lett.* **2024**, *41*, 014205. [CrossRef]
17. Velotta, R.; Hay, N.; Mason, M.; Castillejo, M.; Marangos, J. High-order harmonic generation in aligned molecules. *Phys. Rev. Lett.* **2001**, *87*, 183901. [CrossRef]
18. Zhou, X.; Tong, X.M.; Zhao, Z.; Lin, C.D. Alignment dependence of high-order harmonic generation from N_2 and O_2 molecules in intense laser fields. *Phys. Rev. A* **2005**, *72*, 033412. [CrossRef]
19. Lein, M.; Corso, P.; Marangos, J.P.; Knight, P. Orientation dependence of high-order harmonic generation in molecules. *Phys. Rev. A* **2003**, *67*, 023819. [CrossRef]
20. Vozzi, C.; Calegari, F.; Benedetti, E.; Caumes, J.P.; Sansone, G.; Stagira, S.; Nisoli, M.; Torres, R.; Heesel, E.; Kajumba, N.; et al. Controlling two-center interference in molecular high harmonic generation. *Phys. Rev. Lett.* **2005**, *95*, 153902. [CrossRef]
21. Smirnova, O.; Mairesse, Y.; Patchkovskii, S.; Dudovich, N.; Villeneuve, D.; Corkum, P.; Ivanov, M.Y. High harmonic interferometry of multi-electron dynamics in molecules. *Nature* **2009**, *460*, 972–977. [CrossRef] [PubMed]
22. Fu, T.T.; Zhou, S.S.; Chen, J.G.; Wang, J.; Guo, F.M.; Yang, Y.J. Minimum structure of high-order harmonic spectrum from molecular multi-orbital effects involving inner-shell orbitals. *Opt. Exp.* **2023**, *31*, 30171–30183. [CrossRef] [PubMed]
23. Zhang, B.; Yuan, J.M.; Zhao, Z.X. Dynamic orbitals in high-order harmonic generation from CO molecules. *Phys. Rev. A* **2014**, *90*, 035402. [CrossRef]
24. Miao, X.Y.; Du, H.N. Theoretical study of high-order-harmonic generation from asymmetric diatomic molecules. *Phys. Rev. A* **2013**, *87*, 053403. [CrossRef]
25. Feng, L.; Chu, T. Role of excited states in asymmetric harmonic emission. *Commun. Comput. Chem.* **2013**, *1*, 52–62.
26. Bian, X.B.; Bandrauk, A.D. Nonadiabatic molecular high-order harmonic generation from polar molecules: Spectral redshift. *Phys. Rev. A* **2011**, *83*, 041403. [CrossRef]
27. Li, Y.P.; Yu, S.J.; Li, W.Y.; Chen, Y.J. Orientation dependence of harmonic emission from vibrating HeH^{2+} versus HeT^{2+}: Effects of a permanent dipole. *Phys. Rev. A* **2017**, *95*, 063412. [CrossRef]
28. Bian, X.B.; Bandrauk, A.D. Spectral shifts of nonadiabatic high-order harmonic generation. *Appl. Sci.* **2013**, *3*, 267–277. [CrossRef]
29. Bian, X.B.; Bandrauk, A.D. Orientation dependence of nonadiabatic molecular high-order-harmonic generation from resonant polar molecules. *Phys. Rev. A* **2012**, *86*, 053417. [CrossRef]
30. Hu, H.T.; Li, N.; Liu, P.; Li, R.X.; Xu, Z.Z. Pure even harmonic generation from oriented CO in linearly polarized laser fields. *Phys. Rev. Lett.* **2017**, *119*, 173201. [CrossRef]
31. Long, S.; Becker, W.; McIver, J. Model calculations of polarization-dependent two-color high-harmonic generation. *Phys. Rev. A* **1995**, *52*, 2262. [CrossRef]
32. Levesque, J.; Mairesse, Y.; Dudovich, N.; Pépin, H.; Kieffer, J.C.; Corkum, P.; Villeneuve, D. Polarization state of high-order harmonic emission from aligned molecules. *Phys. Rev. Lett.* **2007**, *99*, 243001. [CrossRef]
33. Li, L.; Lan, P.F.; He, L.X.; Zhu, X.S.; Chen, J.; Lu, P.X. Scaling law of high harmonic generation in the framework of photon channels. *Phys. Rev. Lett.* **2018**, *120*, 223203. [CrossRef] [PubMed]
34. Lambert, G.; Vodungbo, B.; Gautier, J.; Mahieu, B.; Malka, V.; Sebban, S.; Zeitoun, P.; Luning, J.; Perron, J.; Andreev, A.; et al. Towards enabling femtosecond helicity-dependent spectroscopy with high-harmonic sources. *Nat. Commun.* **2015**, *6*, 6167. [CrossRef] [PubMed]
35. Harada, Y.; Haraguchi, E.; Kaneshima, K.; Sekikawa, T. Circular dichroism in high-order harmonic generation from chiral molecules. *Phys. Rev. A* **2018**, *98*, 021401. [CrossRef]
36. Smirnova, O.; Patchkovskii, S.; Mairesse, Y.; Dudovich, N.; Villeneuve, D.; Corkum, P.; Ivanov, M.Y. Attosecond circular dichroism spectroscopy of polyatomic molecules. *Phys. Rev. Lett.* **2009**, *102*, 063601. [CrossRef] [PubMed]
37. Willems, F.; Smeenk, C.; Zhavoronkov, N.; Kornilov, O.; Radu, I.; Schmidbauer, M.; Hanke, M.; von Korff Schmising, C.; Vrakking, M.; Eisebitt, S. Probing ultrafast spin dynamics with high-harmonic magnetic circular dichroism spectroscopy. *Phys. Rev. B* **2015**, *92*, 220405. [CrossRef]
38. Eichmann, H.; Egbert, A.; Nolte, S.; Momma, C.; Wellegehausen, B.; Becker, W.; Long, S.; McIver, J. Polarization-dependent high-order two-color mixing. *Phys. Rev. A* **1995**, *51*, R3414. [CrossRef]
39. Qiao, Y.; Wu, D.; Chen, J.G.; Wang, J.; Guo, F.M.; Yang, Y.J. High-order harmonic generation from H_2^+ irradiated by a co-rotating two-color circularly polarized laser field. *Phys. Rev. A* **2019**, *100*, 063428. [CrossRef]
40. Wang, S.; Cai, J.; Chen, Y.J. Ionization dynamics of polar molecules in strong elliptical laser fields. *Phys. Rev. A* **2017**, *96*, 043413. [CrossRef]
41. Bian, X.B.; Bandrauk, A.D. Phase control of multichannel molecular high-order harmonic generation by the asymmetric diatomic molecule HeH^{2+} in two-color laser fields. *Phys. Rev. A* **2011**, *83*, 023414. [CrossRef]

42. Hermann, M.R.; Fleck, J., Jr. Split-operator spectral method for solving the time-dependent Schrödinger equation in spherical coordinates. *Phys. Rev. A* **1988**, *38*, 6000. [CrossRef] [PubMed]
43. He, F.; Ruiz, C.; Becker, A. Absorbing boundaries in numerical solutions of the time-dependent Schrödinger equation on a grid using exterior complex scaling. *Phys. Rev. A* **2007**, *75*, 053407. [CrossRef]
44. Zhang, X.F.; Zhu, X.S.; Liu, X.; Wang, D.; Zhang, Q.; Lan, P.F.; Lu, P.X. Ellipticity-tunable attosecond XUV pulse generation with a rotating bichromatic circularly polarized laser field. *Opt. Lett.* **2017**, *42*, 1027–1030. [CrossRef] [PubMed]
45. Chu, X.; Chu, S.I. Optimization of high-order harmonic generation by genetic algorithm and wavelet time-frequency analysis of quantum dipole emission. *Phys. Rev. A* **2001**, *64*, 021403. [CrossRef]
46. Milošević, D.B.; Becker, W.; Kopold, R. Generation of circularly polarized high-order harmonics by two-color coplanar field mixing. *Phys. Rev. A* **2000**, *61*, 063403. [CrossRef]